Heliyon 10 (2024) e27450

Contents lists available at ScienceDirect

Heliyon

journal homepage: www.cell.com/heliyon

Research article

Quantitative proteome and lysine succinylome characterization of zinc chloride smoke-induced lung injury in mice

Rui Zhou [a,1], Zhiwei Tu [b,1], Daishi Chen [c,1], Wanmei Wang [d], Shuzi Liu [e], Linjun She [a], Zhan Li [a], Jihong Liu [a], Yabin Li [e], Yu Cui [b,f,**], Pan Pan [e,***], Fei Xie [e,*]

[a] The First Affiliated Hospital of Henan University of Chinese Medicine, 450000, Zhengzhou, Henan, China
[b] National Center for Protein Sciences (Beijing), Institute of Lifeomics, 102206, Beijing, China
[c] Department of Otorhinolaryngology, Shenzhen People's Hospital, Second Clinical Medical College of Jinan University, 515100, Shenzhen, Guangdong, China
[d] Department of Pharmaceutical Sciences, Beijing Institute of Radiation Medicine, 100850, Beijing, China
[e] College of Pulmonary and Critical Care Medicine, The First Medical Center of Chinese PLA General Hospital, 100048, Beijing, China
[f] State Key Laboratory of Proteomics, 102206, Beijing, China

ARTICLE INFO

Keywords:
Lysine succinylation
Ksucc
Succinylome
Lung injury
Zinc chloride smoke

ABSTRACT

The inhalation of zinc chloride ($ZnCl_2$) smoke is one of common resources of lung injury, potentially resulting in severe pulmonary complications and even mortality. The influence of $ZnCl_2$ smoke on lysine succinylation (Ksucc) in the lungs remains uncertain. In this study, we used a $ZnCl_2$ smoke inhalation mouse model to perform global proteomic and lysine succinylome analyses. A total of 6781 Ksucc sites were identified in the lungs, with injured lungs demonstrating a reduction to approximately 2000 Ksucc sites, and 91 proteins exhibiting at least five differences in the number of Ksucc sites. Quantitative analysis revealed variations in expression of 384 proteins and 749 Ksucc sites. The analysis of protein-protein interactions was conducted for proteins displaying differential expression and differentially expressed lysine succinylation. Notably, proteins with altered Ksucc exhibited increased connectivity compared with that in differentially expressed proteins. Beyond metabolic pathways, these highly connected proteins were also involved in lung injury-associated pathological reactions, including processes such as focal adhesion, adherens junction, and complement and coagulation cascades. Collectively, our findings contribute to the understanding of the molecular mechanisms underlaying $ZnCl_2$ smoke-induced lung injury with a specific emphasis on lysine succinylation. These findings could pave the way for targeted interventions and therapeutic strategies to mitigate severe pulmonary complications and mortality associated with such injuries in humans.

Abbreviations: CE, collision energy; DAVID, Database for Annotation Visualization and Integrated Discovery; DEP, differentially expressed proteins; DTT, dithiothreitol; FDR, false discovery rate; IAA, iodoacetamide; ICR, Institute of Cancer Research; IP, immunoprecipitation; LFQ, label-free quantification; MSMS, tandem mass spectrometry; NAM, normalized absolute mean; PASEF, parallel accumulation–serial fragmentation; PBS, phosphate-buffered saline; SDH, succinate dehydrogenase; STRING, Search Tool for the Retrieval of Interacting Genes/Proteins; TCA, tricarboxylic acid; TEAB, tetraethylammonium bromide; TFA, trifluoroacetic acid; TOF, time-of-flight; UHPLC, ultra-high-performance liquid chromatography.

* Corresponding author. College of Pulmonary and Critical Care Medicine, Chinese PLA General Hospital, 100048, Beijing, China.
** Corresponding author. National Center for Protein Sciences (Beijing), Institute of Lifeomics, 102206, Beijing, China.
*** Corresponding author. College of Pulmonary and Critical Care Medicine, Chinese PLA General Hospital, 100048, Beijing, China.
E-mail addresses: cuiyubmi@163.com (Y. Cui), 18701545169@163.com (P. Pan), xiefei0522@163.com (F. Xie).
[1] These authors contributed equally to this work.

https://doi.org/10.1016/j.heliyon.2024.e27450
Received 13 November 2023; Received in revised form 17 January 2024; Accepted 28 February 2024
Available online 8 March 2024

1. Introduction

Inhalation of thermal or chemical irritants, for example zinc chloride ($ZnCl_2$), usually causes lung injury with symptoms of difficulty breathing, asthma, nausea, vomiting, suffocation, and mortality [1,2]. Smoke inhalation is one of the main causes of lung injury [3,4]. Particularly, smoke bombs are frequently employed in military operations and military personnel undergo elevated risks of lung injury than civilians [5,6]. Despite many years of research, the pathogenesis of smoke induced-lung injury has not yet been fully elucidated [4,6–8].

Lysine succinylation (Ksucc), a posttranslational modification discovered in 2011 [8], involves in multiple metabolic pathways and abnormalities of Ksucc associated with various diseases [9–11]. A recent study documented the widespread presence of Ksucc in human lungs [12]. However, whether Ksucc is implicated in molecular changes during lung injury has not been explored.

We aimed to address existing gaps in the literature by employing liquid chromatography–tandem mass spectrometry (LC-MS/MS)-based "omics" strategies to study Ksucc of lung injury in a zinc chloride smoke inhalation mouse model [13]. We sought to identify differentially expressed proteins and Ksucc in the lungs of mice exposure to $ZnCl_2$ and characterize functions of these differentially expressed proteins and proteins with differentially expressed Ksucc sites. Collectively, our findings could provide insights into the molecular mechanisms underlying lung injury, as well as enhance our understanding of the complex processes involved in smoke-induced lung injury, offering a foundation for future research and therapeutic interventions aimed at mitigating the severity of such injuries.

2. Methods

2.1. Collection of biological samples and histopathological validation

A mouse model of lung injury was established following a previously published protocol [13]. Briefly, 6 male Institute of Cancer Research (ICR) mice (25 ± 2 g, SPF Biotechnology Co. Ltd. Beijing, China) were randomly assigned to two groups (n = 3 per group). One group served as the healthy control, whereas the other was exposed in a smoke-producing experimental chamber (1 m × 0.8 m × 0.6 m) with a 3 g smoke bomb ignition. The mice were removed from the cage after 3 min. After 48 h, the mice were euthanized and dissected. The lungs were excised and the upper lobes of the right lungs were immersed in 10% (v/v) formalin, embedded in paraffin, sliced, stained with hematoxylin and eosin (H&E), and observed under a light microscope. The left lung was used for proteomic analysis. All experimental procedures and animal welfare protocols adhered to the National Institute of Heahth guidelines for laboratory animal care.

2.2. Sample preparation for LC-MS/MS

Fresh samples were rinsed three times in pre-cooled phosphate-buffered saline (PBS) to remove blood. Approximately 50 mg of lung tissue was pulverized in a liquid nitrogen-cooled mortar. 200 μl lysis buffer [8 M urea (Sigma-Aldrich, Saint Louis, USA), 1% (w/v) protease inhibitor (Merck Millipore, Saint Louis, USA), 2 μM trichostain A (TSA) (MedChemExpress, South Brunswick, USA), and 50 mM N-acetylmuramic acid (NAM) (Sigma-Aldrich, Saint Louis, USA)] was added to re-suspend samples, followed by ultrasonication. After centrifugation at 12,000 g, 4 °C for 10 min, the supernatant was transferred to a clean Eppendorf tube. Proteins (500 mg) were precipitated by adding 20% (v/v) trichloroacetic acid (TFA) (Sigma-Aldrich, Saint Louis, USA) and vertexing for 2 h. Samples were centrifuged at 4500 g for 5 min and the supernatant was discarded. The pellet was washed three times with pre-cooled acetone (Hangzhou Hannuo Chemical Co., Ltd., Hangzhou, China) and vacuum dried. Proteins were re-suspended in 200 mM tetraethylammonium bromide (TEAB) (Sigma-Aldrich, Saint Louis, USA) and dithiothreitol (DTT) (Sigma-Aldrich, Saint Louis, USA) was added to a final concentration of 5 mM and this solution was incubated at 56 °C for 30 min. Iodoacetamide (IAA, Sigma-Aldrich, Saint Louis, USA) was then added to a final concentration of 20 mM, and the mixture was incubated in the dark for 15 min at room temperature. Trypsin (Promega, Madison, USA) was added in a protease: protein (w/w) ratio of 1:30 to digest protein overnight at 37 °C and the peptides were ready for proteome analysis.

Vacuum dried peptides were dissolved in immunoprecipitation (IP) buffer (100 mM NaCl, 1 mM EDTA (Sigma-Aldrich, Saint Louis, USA), 50 mM Tris-HCl, and 0.5% (v/v) NP-40; pH 8.0) and incubated with a resin coated with anti-succinyl antibodies (Antibody Resin No. Ptm-402; Hangzhou Jingjie Biotechnology Co. Ltd., Hangzhou, China) overnight at 4 °C on a rotating shaker. The next day, the resin was washed four times with the IP buffer and rinsed twice with deionized water. The enriched peptides were eluted with 0.1% (v/v) TFA and freeze-dried. Peptide cleanup was performed using homemade C18 tip columns.

2.3. LC-M/MS

Peptides were dissolved in 0.1% formic acid and 200 ng equivalent was injected into a self-packed C18 analytical column (100 μm x 300 mm) kept at 50 °C using the nanoElute UHPLC system (Bruker, Bremen, Germany). The peptides were eluted at a flow rate of 450 nl/min with a multi-step gradient [solvent A: 0.1% formic acid (Fluka, Saint Louis, USA) in water, solvent B: 0.1% formic acid in acetonitrile (ThermoFisher Scientific, Waltham, USA)] to 6% B at 0 min, 24% B at 70 min, 35% B at 84 min, 80% B at 87 min held until 90 min. A shorter elution gradient was used for the analysis of the Ksucc peptides: to 6% B at 0 min, 22% B at 43 min, 30% B at 56 min, 80% B at 58 min held until 60 min.

Eluted peptides were sprayed by the emitter coupled to the column into a captive spray source with a capillary voltage of 1.75 kV, a source gas flow of 3 L/min of nitrogen and a dry temperature of 180 °C, attached to a timsTOF pro 2 mass spectrometer (Bruker, Bremen Germany). The TOF scan range was 100–1700 m/z and 1/K0 = 0.75–1.40 V s/cm^2. The timsTOF was operated in the parallel accumulation–serial fragmentation (PASEF) mode of acquisition. Precursors above the minimum intensity threshold of 2500 were isolated with 2 Th at < 700 m/z or 3 Th > 800 m/z and the target intensity was 10,000 considering a dynamic exclusion of 30 s. The collision energy (CE) was uplifted as increasing mobility starting from 20 eV at 1/K0 = 0.6 V s/cm^2 to 59 eV at 1/K0 = 1.6 V s/cm^2. Ten PASEF MS/MS scans were scheduled, and a charge state range of 0–5 was used. The complete mass spectrometry method is presented in Supplementary File S1. The mass spectrometry method for Ksucc samples is presented in Supplementary File S2. The TOF 1/K0 range was 0.7–1.2 V s/cm^2. The precursor target intensity was 20,000 and the dynamic exclusion was 24 s. The remainder of the method was the same as described earlier.

2.4. Data processing and bioinformatic analysis

MaxQuant (version 1.6.15) was used to process raw MS data [14]. The *Mus musculus* proteome database was acquired from Uniprot (https://www.uniprot.org/) with proteome ID UP000000589 on December 14, 2020 [15]. The digestion enzyme was trypsin/P, with a maximum of two missed cleavages. The minimum peptide length was seven. Cysteine carbamidomethylation was set as a fixed modification, and methionine oxidation and acetylation of the protein N-terminus were set as variable modifications, with a maximum of five modification sites per peptide. The mass tolerance for both precursor and fragment ions was set to 20 ppm. False discovery rate (FDR) was controlled to 1% for peptides and proteins. LFQ quantification and match between run were enabled. The other parameters were set to default values. R software version 4.2.2 (https://www.r-project.org/) was used to process the proteinGroups.txt of MaxQuant outputs. Potential contaminants and reverse proteins were excluded. Proteins identified at least twice in three biological replicates were subjected to further analyses. The relative expression quantity (R) of proteins was calculated by centralizing the LFQ intensity (I) according to equation (1), where *i* represents the samples and *j* represents the proteins.

$$R_{ij} = I_{ij} \,/\, Mean(I_j) \tag{1}$$

The fold change in protein expression was calculated using the average value of the relative expression of biological replicates in one condition divided by the average value of the relative expression of biological replicates in the other condition. Student's t-test was used to calculate the p-value, and the FDR was controlled using the Benjamini–Hochberg procedure [16].

A similar MaxQuant search was performed on the raw MS data for lysine succinylation. Additionally, succinylation on lysine was set as an extra variable modification. Digestion enzyme was trypsin/P with a maximum of four missed cleavages. The Succi (K)Sites.txt of MaxQuant outputs was used for further analysis. Potential contaminants and reverse sites were removed from the results. The localization probability cutoff for lysine succinylation was 0.75. Ksucc sites identified at least twice in three biological replicates were subjected to further analyses. The relative expression quantity (R) of Ksucc sites was calculated by centralizing the intensity (I) according to equation (1), where *i* represents the samples and *j* represents the Ksucc sites. Normalized relative expression quantity (NR) was calculated according to equation (2).

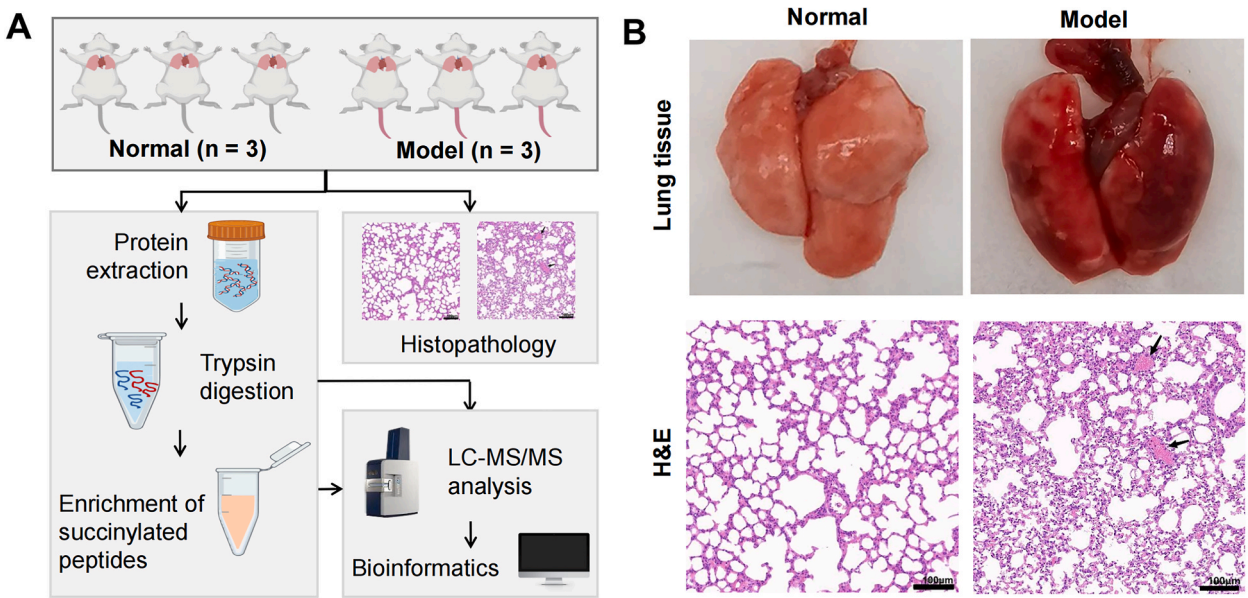

Fig. 1. Overall workflow and histopathology. A. Schematic workflow of the study. B. General appearance of the lungs and H&E staining of the histological sections. Arrows indicate regions of alveolar hemorrhage.

$$NR_{ij} = R_{ij} \,/\, Median(R_i) \quad (2)$$

To mitigate the impact of protein expression on the quantification of Ksucc sites, the normalized relative expression of Ksucc sites was divided by the relative expression of the corresponding proteins. The calculation of the Ksucc site expression fold change and statistical p-value followed the same procedure as described earlier. Differentially expressed proteins or Ksucc sites were defined as having a fold change greater than 1.5 and an adjusted p value less than 0.05, unless otherwise stated.

The online software MoMo version 5.5.0 (https://meme-suite.org/meme/tools/momo) was utilized to discover sequence motifs associated with Ksucc [17]. Protein-protein interaction analysis was performed using the STRING 11.5 database (http://www.string-db.org) with a minimum interaction score of 0.9 [18]. The interactions were visualized using Cytoscape 3.9.1 [19]. DAVID Bioinformatics Resources tool (version 2021) was used to retrieve Gothe Gene Ontology (GO) and Kyoto Encyclopedia of Genes and Genomes (KEGG) pathway enrichment of proteins [20,21].

3. Results

3.1. Workflow for proteomic and lysine succinylome analysis and histopathology

We previously established a mouse model of lung injury induced by zinc chloride smoke inhalation [13]. To comprehensively map the proteome and succinylome changes in injured lungs, we performed LC-MS/MS-based proteome and lysine succinylation analyses on both normal and injured lung tissues. The workflow of the study is illustrated in Fig. 1A. Before further analysis of lung tissues, we monitored and confirmed the histopathological changes (Fig. 1B). The injured lungs exhibited a dark red color and signs of pulmonary oedema. H&E staining of histological sections revealed noticeable pulmonary interstitial oedema and minor hemorrhage. These changes were consistent with that observed in a previous study [13].

3.2. Identification of proteome and lysine succinylation

The tryptic samples underwent LC-MS/MS analysis to identify the proteomes of lungs exposed to $ZnCl_2$ smoke and those without exposure. A total number of 6484 and 6503 proteins were identified in the model (M) and normal (N) samples, respectively, with at least two identifications out of three replicates (Fig. 2A, refer to Supplementary Table S1 for a proteomic study summary). Approximately 97% (6401) of the identified proteins were common to both normal and model samples (Fig. 2B). Pearson's correlation analysis yielded a minimum r of 0.971 (Supplementary Fig. S1), indicating the proteomics analysis system was robust (including Supplementary Table S1).

Ksucc peptides were enriched from the digests and analyzed using LC-MS/MS. Approximately 14000 peptides were identified from

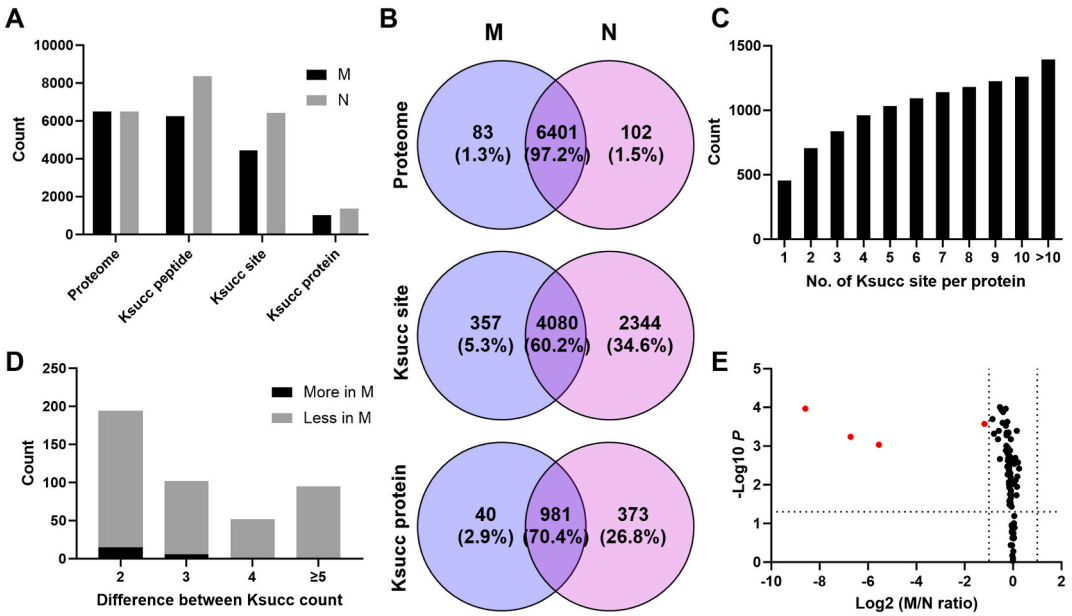

Fig. 2. Identification summary of proteome and lysine succinylation. A. Bar plot for the identification of proteins, Ksucc peptides, sites and proteins. B. Venn diagram of the identified proteins, Ksucc sites and Ksucc proteins in normal(N) and model tissues (M). C. Bar plot of the cumulative counts of proteins with different number of Ksucc sites. D. Bar plot for the number of proteins with certain differences in the number of Ksucc sites between the normal and model Ksucc proteins. E. Volcano plot for proteins exhibiting a minimum of 5 Ksucc site differences. Red dots indicate a protein expression ratio greater than two-fold.

each sample. However, 45% of the peptides in model samples and 54% in normal samples are lysine succinylated with a localization probability >0.75 (see Supplementary Table S2 for identification summary), resulting in 4437 (M) and 6424 (N) Ksucc sites, i.e., 1021 (M) and 1354 (N) Ksucc proteins (Fig. 2A). A typical MS/MS spectrum of the Ksucc peptide identified in the patty acid beta-oxidation enzyme, Hadha, is presented in Supplementary Fig. S2. Over 2000 Ksucc sites and 300 Ksucc proteins were exclusively identified in normal samples, accounting for one-third of the total Ksucc sites and one-fourth of the total Ksucc proteins (Fig. 2B). Multiple Ksucc sites were identified in several proteins (Fig. 2C), which is consistent with previous studies on lysine succinylation [22,23]. Moreover, exposure to $ZnCl_2$ smoke reduced the number of Ksucc sites in some proteins (Fig. 2D). Among proteins with at least five Ksucc site difference, most revealed a protein expression ratio within two-fold (Fig. 2E, based on proteome data, see below for more results), which could partially explain why the reduced number of Ksucc sites was not owing to downregulation of their proteins.

3.3. Quantification of proteome and lysine succinylation

Label-free quantification (LFQ) was performed on both the proteome and succinylome data. Of the 5500 quantified proteins (proteome data) and 4020 Ksucc sites, 384 proteins and 749 Ksucc sites were significantly differentially expressed (Supplementary Fig. S3, Supplementary Tables S3 and S4). Fig. 3A depicts the M/N ratios of Ksucc site and their corresponding protein ratios. This indicates that succinylation displayed larger fluctuations than their respective proteins. the proteins and enzymes involved in the regulation of lysine succinylation were examined. Succinate dehydrogenase (SDH), histone acetyltransferase 1 (hat1) and dihydrolipoyl succinyltransferase (E2k, Dlst in mice) could regulate succinylation by affecting the accumulation of succinyl CoA [24–28]. We detected a significant difference in the expression of Hat1, E2k, and the subunits of SDH (Fig. 3B). These proteins may play a role in regulating succinylation in response to $ZnCl_2$ smoke exposure. Other succinylation regulators, such as Sirt5 [29], Cpt1A [30], and Ogdh [31], did not show significant differences in protein expression. A similar proteomic study was performed in rats [32]. The authors investigated the proteomic changes in the lungs after $ZnCl_2$ smoke inhalation. Of the 27 DEPs, we identified 12 with identical regulation and nine with differential regulation (Supplementary Table S5).

3.4. Identification of lysine succinylation motifs

Amino acid sequences around the Ksucc sites may exhibit certain preferences under different conditions. Hence, the motif-x algorithm was used to detect Ksucc motifs [17]. Six conserved motifs were identified among the sequences surrounding all the identified Ksucc sites (Fig. 4A). Alanine (A), Glutamic Acid (E), glycine (G), lysine (K), arginine (R) and valine (V) were the most common residues surrounding Ksucc sites. Two conserved motifs were identified in the sequence around the Ksucc sites with significantly differential expression (Fig. 4B), with lysine (K) and arginine (R) was the most prominent residues.

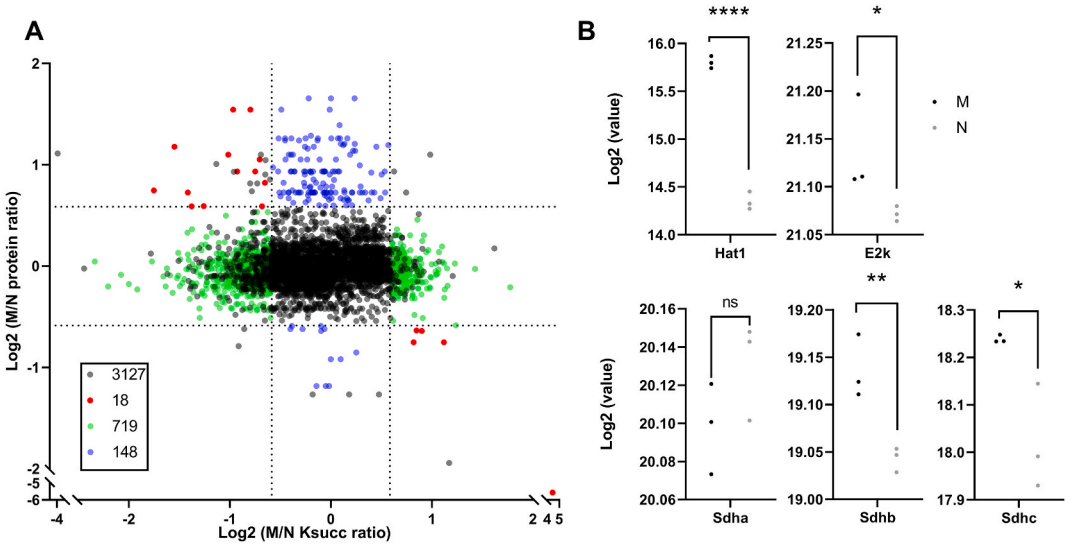

Fig. 3. Overview of expression of lysine succinylation and their putative regulators. A. Scatter plot of the expression of Ksucc sites and their corresponding proteins. Dashed lines indicate an expression fold change of 1.5 (M/N ratio = 1.5 or N/M ratio = 1.5). DEPs or Ksucc sites were defined as expression fold change >1.5 and p value < 0.05. Dots in gray indicate that the expression is not significant for both Ksucc and proteins. Blue indicates the significant expression was only occurred to proteins. Dots in green represents significant expression for Ksucc only. Dots in red state the protein and Ksucc are both significantly differentially expressed. The number of proteins in different classifications is shown in the plot. B. Expression of Ksucc regulators Hat1, E2k and subunits of SDH. ns, not significant; *, $p < 0.05$; **, $p < 0.01$; ****, $p < 0.0001$.

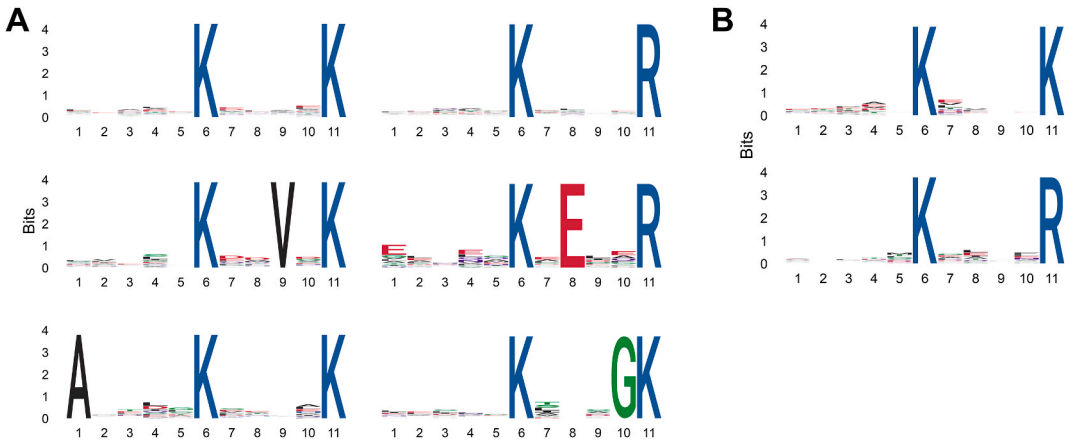

Fig. 4. Motif analysis of succinylated peptides. A. Conserved motifs identified from sequences surrounding all identified Ksucc sites. B. Conserved motifs identified from sequences surrounding Ksucc sites with differential expression.

3.5. *Functional analysis of proteins with fewer ksucc sites, DEPs, and DEKsuccs*

A total of 803 proteins were involved in the functional analysis, including proteins exhibiting a minimum of 5 Ksucc site differences and an expression fold change of the corresponding protein smaller than 2 after exposure to $ZnCl_2$ smoke (PLKsuccs), differentially expressed proteins (DEPs) and proteins with differentially expressed Ksucc sites (DEKsuccs). Some proteins were repeated when characterizing them into three classes (Fig. 5A). These proteins were mainly found in the cytoplasm, extracellular regions and mitochondria (Supplementary Fig. S4A). Molecular function analysis indicated that they possessed oxidoreductase and peptidase activities and binding properties to proteins, nucleotides, and actins (Supplementary Fig. S4B). GO biological process and KEGG

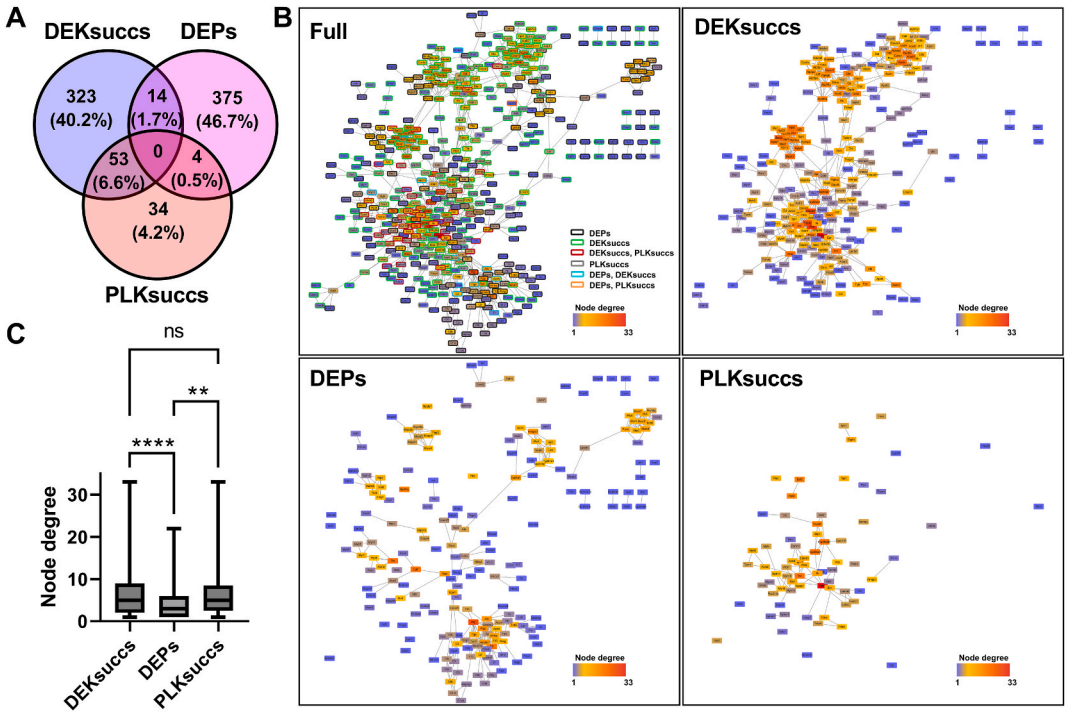

Fig. 5. Protein-protein interaction analysis of proteins with fewer Ksucc sites (PLKsuccs), differentially expressed proteins (DEPs) and proteins with differentially expressed Ksucc sites (DEKsuccs). A. Venn diagram of proteins of three groups. B. Protein-protein interaction network of proteins of three group. A full network in these proteins of three groups is displayed. Nodes represent proteins, and edges indicate that the proteins were connected in the analysis with a minimum interaction score of 0.9. The color of the nodes is represents the number of proteins connected (degree) according to the legend. The border of nodes is colored to indicate the classification of three groups. C. Box plot for the degrees of proteins in three groups. ns, not significant; **, $p < 0.01$; ****, $p < 0.0001$.

pathway analysis indicated they were involved in focal adhesion, nucleosome assembly, blood coagulation, as well as the metabolism of amino acids, carbon, fatty acids, and lipids (Supplementary Figs. S4C and S4D).

Protein-protein interaction information was obtained from the STRING database (http://string-db.org/) to analyze the correlations between these proteins [18]. A total of 497 proteins displayed at least one connection with other proteins (Fig. 5B). Additionally, proteins with alterations in Ksucc from either DEKsuccs or PLKsuccs had higher levels of protein-protein interactions than those from DEPs (Fig. 5B and C). Subsequently, we focused on proteins with a higher level of connectivity, i.e., proteins with node degrees $\geq$8, as they may have more important roles. These proteins were involved in several metabolic and functional pathways (Fig. 6). Details of the highly connected proteins that were not enriched in the functional pathways are listed in Table 1. It is conceivable that different regulatory ways act together to regulate a specific pathway, such as carbon metabolism; some proteins have fewer Ksucc sites, and some proteins are differentially expressed in Ksucc. These functional pathways also interact with each other through shared proteins and connections, as indicated by the STRING database. Among these, DNA replication proteins were independent of the others and comprised only DEPs.

4. Discussion

Smoke inhalation is frequently encountered during fire disasters, military operations, and exposure to toxic chemical gases [53]. Over one–fifth of burn patients endure lung injuries caused by smoke inhalation, contributing to 30% of fire related fatalities [53,54]. Moreover, military personnel are at significant risk of smoke inhalation–induced lung injury during the deployment of smoke bombs, which commonly contain $ZnCl_2$ as the main component [5,6,55]. The incidence of clinical cases related to smoke bomb-induced lung injuries has been steadily increasing since 1945 [56]. To enhance our understanding of the molecular mechanisms underlying lung injury induced by zinc chloride, we established a robust mouse model of lung injury induced by smoke bombs containing zinc chloride as the primary component [13]. In this study, we elucidated the role of lysine succinylation in $ZnCl_2$-injured lungs for the first time. Approximately 2000 Ksucc sites were not identified in the injured lungs, potentially owing to succinylation occurring at an ultra-low level beyond the detection limit of the mass spectrometer or even complete de-succinylation. Regardless of the condition, Ksucc level on lysine were downregulated in response to the smoke stimulation. Over 60% of the Ksucc sites were identified and quantified in both normal and injured lungs. Ksucc displayed a larger dynamic range of up- or down-regulation compared with the expression of their corresponding proteins, indicating a more pronounced response of Ksucc in lung injury.

Additionally, STRING analysis revealed a higher protein-protein connectivity of Ksucc proteins, suggesting a potentially distinct or more critical role of Ksucc in lung injury induced by zinc chloride smoke. Two conserved residues, arginine (R) and lysine (K) constitute the Ksucc motif in the lungs of human [12]. While we also identified them during our analysis of mouse models, their positions were two amino acids closer to the Ksucc sites. Minor differences between the two species are reasonable and expected. Nevertheless, the results of this study provide insights for investigating zinc chloride smoke–induced lung injury in humans.

Protein lysine succinylation occurs across various subcellular locations, including the cytosol, mitochondria, and nucleus, as well as in enzymes participating in metabolic pathways related to processed such as fatty acid synthesis, amino acid degradation, and the TCA cycle [57–59]. Our findings align with existing literature. Furthermore, proteins with high connectivity are implicated in focal adhesion, adherens junctions, complement and coagulation cascades. These functional pathways play a role in pathological reactions to lung injury [60]. However, further investigation is necessary to confirm the role of Ksucc in these proteins in responses to the inhalation of zinc chloride smoke. Proteins, mRNAs and signaling pathways have been reported to associate with adherens junctions, pulmonary epithelial barrier dysfunction and abnormal coagulation reaction in smoke induced lung injury [61–65] and protein phosphorylation has been reported in ventilator-induced lung injury [66]. However, our study is the first to elucidate the involvement of Ksucc in smoke-induced lung injury.

The study's findings may hold significant implications for clinical practice, especially in the context of military professionals exposed to smoke bombs containing zinc chloride. Understanding the molecular mechanisms, specifically lysine succinylation, associated with lung injury induced by such exposure could pave the way for targeted therapeutic interventions. This insight may guide the development of novel treatments or preventive measures tailored to mitigate the impact of smoke-induced lung injuries in military personnel. By elucidating the role of Ksucc in the pathological responses to zinc chloride smoke, the study may contribute to improved medical strategies and healthcare practices for addressing lung injuries in a military setting. This knowledge could potentially enhance the overall health and well-being of military professionals facing the risk of smoke inhalation during operations involving the deployment of smoke bombs.

Ethics statement

This study was reviewed and approved by the Animal Ethics Committee of the Institute of Automation of the Chinese Academy of Sciences, with the approval number: IA21-2203-10.

Data availability statement

The raw proteomics data have been deposited to the MassIVE repository with the data set identification number MSV000090800 (username: MSV000090800_reviewer, password: 147258).

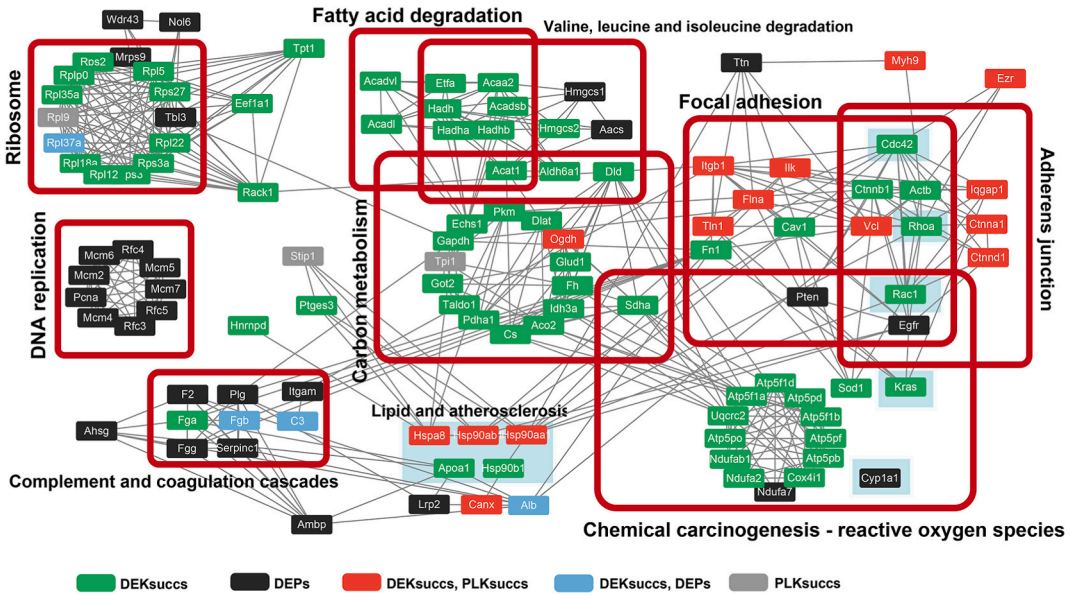

Fig. 6. Protein-protein interaction network of proteins with node ≥8. Nodes represent proteins, and edges indicate a connection in STRING analysis. The color of nodes specifies the classification of proteins as depicted in the plot. Proteins enriched in KEGG pathways are highlighted using a dark red square or filled with an identical background color.

Table 1
Proteins with high connectivity but not enriched in KEGG pathways.

Protein	Function	Reference
Wdr43	Associated with ribosome biogenesis and colorectal cancer	[33,34]
No16	Promote cell proliferation and inhibit apoptosis	[35]
Tpt1	Negatively regulates autophagy	[36]
Eef1a1	Enhance oncogenesis, block apoptosis, and increase viral pathogenesis	[37]
Rack1	Participate airway epithelial mesenchymal transition and apoptosis	[38]
Ttn	Increase right ventricular diastolic stiffness in pulmonary arterial hypertension	[39]
Myh9	Involve in cytoskeleton reorganization	[40]
Ezr	Promote cancer cell migration and lymph node metastasis	[41]
Stip1	Inhibit glycolysis and participate in cancer tumorigenesis and progression	[42,43]
Ptges3	Involve in cell cycle and act as an independent predictive prognostic in lung adenocarcinoma	[44]
Hnrnpd	Antagonizes ferroptosis and alleviate sepsis-induced acute lung injury	[45]
Ahsg	Promotes the proliferation of bladder cancer cells	[46]
Ambp	Attenuate vascular endothelial cell apoptosis in sepsis	[47]
Lrp2	Regulating muscle glucose metabolism and insulin sensitivity	[48]
Canx	Participate in collagen degradation of idiopathic pulmonary fibrosis	[49]
Alb	Increase antioxidant capacity, protects against lung injury	[50–52]

Funding

This study was supported by the Military Program (No. BLB20J002), the National Key Research Program of China (No. 2019YFC0121703), and the National Natural Science Foundation of China (No. 61976223).

CRediT authorship contribution statement

Rui Zhou: Writing – review & editing, Writing – original draft, Investigation. **Zhiwei Tu:** Writing – review & editing, Investigation. **Daishi Chen:** Writing – original draft. **Wanmei Wang:** Data curation. **Shuzi Liu:** Data curation. **Linjun She:** Visualization, Dr. **Zhan Li:** Validation. **Jihong Liu:** Visualization. **Yabin Li:** Validation. **Yu Cui:** Conceptualization. **Pan Pan:** Conceptualization. **Fei Xie:** Supervision, Project administration, Funding acquisition, Conceptualization.

Declaration of competing interest

The authors declare that they have no known competing financial interests or personal relationships that could have appeared to influence the work reported in this paper.

Acknowledgments

We appreciate the technical support of Mr. Bin Fu and Miss Shuhui Ji from the National Center for Protein Sciences (Beijing).

Appendix A. Supplementary data

Supplementary data to this article can be found online at https://doi.org/10.1016/j.heliyon.2024.e27450.

References

[1] S. Rehberg, M.O. Maybauer, P. Enkhbaatar, D.M. Maybauer, Y. Yamamoto, D.L. Traber, Pathophysiology, management and treatment of smoke inhalation injury, Expert Rev Respir Med 3 (2009) 283–297, https://doi.org/10.1586/ERS.09.21.
[2] K.Z. Shirani, B.A. Pruitt Jr., A.D. Mason Jr., The influence of inhalation injury and pneumonia on burn mortality, Ann. Surg. 205 (1987) 82–87, https://doi.org/10.1097/00000658-198701000-00015.
[3] A.S. Lee, R.B. Mellins, Lung injury from smoke inhalation, Paediatr. Respir. Rev. 7 (2006) 123–128, https://doi.org/10.1016/j.prrv.2006.03.003.
[4] B. Guo, Y. Bai, Y. Ma, C. Liu, S. Wang, R. Zhao, J. Dong, H.-L. Ji, Preclinical and clinical studies of smoke-inhalation-induced acute lung injury: update on both pathogenesis and innovative therapy, Ther. Adv. Respir. Dis. 13 (2019) 1753466619847901, https://doi.org/10.1177/1753466619847901.
[5] F. Xie, X. Zhang, L. Xie, Prognostic value of serum zinc levels in patients with acute HC/zinc chloride smoke inhalation, Medicine (Baltim.) 96 (2017) e8156, https://doi.org/10.1097/MD.0000000000008156.
[6] L. Cao, X.G. Zhang, J.G. Wang, H.B. Wang, Y.B. Chen, D.H. Zhao, W.F. Shi, L.X. Xie, Pulmonary function test findings in patients with acute inhalation injury caused by smoke bombs, J. Thorac. Dis. 8 (2016) 3160–3167, https://doi.org/10.21037/jtd.2016.11.94.
[7] F. Zhang, M.Y. Li, Y.T. Lan, C.B. Wang, Imbalance of Th17/Tregs in rats with smoke inhalation-induced acute lung injury, Sci. Rep. 6 (2016) 21348, https://doi.org/10.1038/srep21348.
[8] Z.H. Zhang, M.J. Tan, Z.Y. Xie, L.Z. Dai, Y. Chen, Y.M. Zhao, Identification of lysine succinylation as a new post-translational modification, Nat. Chem. Biol. 7 (2011) 58–63, https://doi.org/10.1038/Nchembio.495.
[9] J. Park, Y. Chen, D.X. Tishkoff, C. Peng, M.J. Tan, L.Z. Dai, Z.Y. Xie, Y. Zhang, B.M.M. Zwaans, M.E. Skinner, D.B. Lombard, Y.M. Zhao, SIRT5-Mediated lysine desuccinylation impacts diverse metabolic pathways, Mol Cell 50 (2013) 919–930, https://doi.org/10.1016/j.molcel.2013.06.001.
[10] M.J. Rardin, W.J. He, Y. Nishida, J.C. Newman, C. Carrico, S.R. Danielson, A. Guo, P. Gut, A.K. Sahu, B. Li, R. Uppala, M. Fitch, T. Riiff, L. Zhu, J. Zhou, D. Mulhern, R.D. Stevens, O.R. Ilkayeva, C.B. Newgard, M.P. Jacobson, M. Hellerstein, E.S. Goetzman, B.W. Gibson, E. Verdin, SIRT5 regulates the mitochondrial lysine succinylome and metabolic networks, Cell Metab 18 (2013) 920–933, https://doi.org/10.1016/j.cmet.2013.11.013.
[11] C. Diskin, T.A.J. Ryan, L.A.J. O'Neill, Modification of proteins by metabolites in immunity, Immunity 54 (2021) 19–31, https://doi.org/10.1016/j.immuni.2020.09.014.
[12] Y.H. Yang, S.F. Wu, Y.P. Zhu, J.T. Yang, J.F. Liu, Global profiling of lysine succinylation in human lungs, Proteomics 22 (2022), https://doi.org/10.1002/pmic.202100381. ARTN e2100381.
[13] W. Wang, Y. Liu, P. Pan, Y. Huang, T. Chen, T. Yuan, Y. Ma, G. Han, J. Li, Y. Jin, F. Xie, Pulmonary delivery of resveratrol-β-cyclodextrin inclusion complexes for the prevention of zinc chloride smoke-induced acute lung injury, Drug Deliv. 29 (2022) 1122–1131, https://doi.org/10.1080/10717544.2022.2048135.
[14] S. Tyanova, T. Temu, J. Cox, The MaxQuant computational platform for mass spectrometry-based shotgun proteomics, Nat. Protoc. 11 (2016) 2301–2319, https://doi.org/10.1038/nprot.2016.136.
[15] D.M. Church, L. Goodstadt, L.W. Hillier, M.C. Zody, S. Goldstein, X. She, C.J. Bult, R. Agarwala, J.L. Cherry, M. DiCuccio, W. Hlavina, Y. Kapustin, P. Meric, D. Maglott, Z. Birtle, A.C. Marques, T. Graves, S. Zhou, B. Teague, K. Potamousis, C. Churas, M. Place, J. Herschleb, R. Runnheim, D. Forrest, J. Amos-Landgraf, D.C. Schwartz, Z. Cheng, K. Lindblad-Toh, E.E. Eichler, C.P. Ponting, C. Mouse Genome Sequencing, Lineage-specific biology revealed by a finished genome assembly of the mouse, PLoS Biol. 7 (2009) e1000112, https://doi.org/10.1371/journal.pbio.1000112.
[16] Y. Benjamini, Y. Hochberg, Controlling the false discovery rate, A Practical and Powerful Approach to Multiple Testing 57 (1995) 289–300.
[17] A. Cheng, C.E. Grant, W.S. Noble, T.L. Bailey, MoMo: discovery of statistically significant post-translational modification motifs, Bioinformatics 35 (2019) 2774–2782, https://doi.org/10.1093/bioinformatics/bty1058.
[18] D. Szklarczyk, A.L. Gable, D. Lyon, A. Junge, S. Wyder, J. Huerta-Cepas, M. Simonovic, N.T. Doncheva, J.H. Morris, P. Bork, L.J. Jensen, C.v. Mering, STRING v11: protein-protein association networks with increased coverage, supporting functional discovery in genome-wide experimental datasets, Nucleic Acids Res. 47 (2019) D607–D613, https://doi.org/10.1093/nar/gky1131.
[19] P. Shannon, A. Markiel, O. Ozier, N.S. Baliga, J.T. Wang, D. Ramage, N. Amin, B. Schwikowski, T. Ideker, Cytoscape: a software environment for integrated models of biomolecular interaction networks, Genome Res. 13 (2003) 2498–2504, https://doi.org/10.1101/gr.1239303.
[20] W. Huang da, B.T. Sherman, R.A. Lempicki, Systematic and integrative analysis of large gene lists using DAVID bioinformatics resources, Nat. Protoc. 4 (2009) 44–57, https://doi.org/10.1038/nprot.2008.211.
[21] W. Huang da, B.T. Sherman, R.A. Lempicki, Bioinformatics enrichment tools: paths toward the comprehensive functional analysis of large gene lists, Nucleic Acids Res. 37 (2009) 1–13, https://doi.org/10.1093/nar/gkn923.
[22] F. Sun, X. Huo, Y. Zhai, A. Wang, J. Xu, D. Su, M. Bartlam, Z. Rao, Crystal structure of mitochondrial respiratory membrane protein complex II, Cell 121 (2005) 1043–1057, https://doi.org/10.1016/j.cell.2005.05.025.
[23] S. Ren, M. Yang, Y. Yue, F. Ge, Y. Li, X. Guo, J. Zhang, F. Zhang, X. Nie, S. Wang, Lysine succinylation contributes to aflatoxin production and pathogenicity in Aspergillus flavus, Mol. Cell. Proteomics 17 (2018) 457–471, https://doi.org/10.1074/mcp.RA117.000393.
[24] J. Smestad, L. Erber, Y. Chen, L.J. Maher, Chromatin succinylation correlates with active gene expression and is perturbed by defective TCA cycle metabolism, iScience 2 (2018) 63, https://doi.org/10.1016/j.isci.2018.03.012.
[25] F. Li, X.D. He, D.W. Ye, Y. Lin, H.X. Yu, C.F. Yao, L. Huang, J.N. Zhang, F. Wang, S. Xu, X.H. Wu, L.X. Liu, C. Yang, J.Q. Shi, X.Y. He, J. Liu, Y.Y. Qu, F.S. Guo, J. Y. Zhao, W. Xu, S.M. Zhao, NADP(+)-IDH mutations promote hypersuccinylation that impairs mitochondria respiration and induces apoptosis resistance, Mol Cell 60 (2015) 661–675, https://doi.org/10.1016/j.molcel.2015.10.017.
[26] G.E. Gibson, H. Xu, H.L. Chen, W. Chen, T.T. Denton, S. Zhang, Alpha-ketoglutarate dehydrogenase complex-dependent succinylation of proteins in neurons and neuronal cell lines, J. Neurochem. 134 (2015) 86–96, https://doi.org/10.1111/jnc.13096.
[27] R.A.W. Frank, A.J. Price, F.D. Northrop, R.N. Perham, B.F. Luisi, Crystal structure of the E1 component of the Escherichia coli 2-oxoglutarate dehydrogenase multienzyme complex, J. Mol. Biol. 368 (2007) 639–651, https://doi.org/10.1016/j.jmb.2007.01.080.
[28] G. Yang, Y. Yuan, H.F. Yuan, J.P. Wang, H.L. Yun, Y. Geng, M. Zhao, L.H. Li, Y.J. Weng, Z.X. Liu, J.Y. Feng, Y.N. Bu, L. Liu, B.N. Wang, X.D. Zhang, Histone acetyltransferase 1 is a succinyltransferase for histones and non-histones and promotes tumorigenesis, EMBO Rep. 22 (2021), https://doi.org/10.15252/embr.202050967. ARTN e50967.
[29] J.T. Du, Y.Y. Zhou, X.Y. Su, J.J. Yu, S. Khan, H. Jiang, J. Kim, J. Woo, J.H. Kim, B.H. Choi, B. He, W. Chen, S. Zhang, R.A. Cerione, J. Auwerx, Q. Hao, H.N. Lin, Sirt5 is a NAD-dependent protein lysine demalonylase and desuccinylase, Science 334 (2011) 806–809, https://doi.org/10.1126/science.1207861.

[30] X. Li, C. Zhang, T. Zhao, Z.P. Su, M.J. Li, J.C. Hu, J.F. Wen, J.J. Shen, C. Wang, J.S. Pan, X.M. Mu, T. Ling, Y.C. Li, H. Wen, X.R. Zhang, Q. You, Lysine-222 succinylation reduces lysosomal degradation of lactate dehydrogenase a and is increased in gastric cancer, J Exp Clin Canc Res 39 (2020), https://doi.org/10.1186/s13046-020-01681-0. ARTN 172.
[31] B. Nagy, M. Polak, O. Ozohanics, Z. Zambo, E. Szabo, A. Hubert, F. Jordan, J. Nováček, V. Adam-Vizi, A. Ambrus, Structure of the dihydrolipoamide succinyltransferase (E2) component of the human alpha-ketoglutarate dehydrogenase complex (hKGDHc) revealed by cryo-EM and cross-linking mass spectrometry: implications for the overall hKGDHc structure, Biochim. Biophys. Acta Gen. Subj. 1865 (2021) 129889, https://doi.org/10.1016/j.bbagen.2021.129889.
[32] X. Xie, J. Zhao, L. Xie, H. Wang, Y. Xiao, Y. She, L. Ma, Identification of differentially expressed proteins in the injured lung from zinc chloride smoke inhalation based on proteomics analysis, Respir. Res. 20 (2019) 36, https://doi.org/10.1186/s12931-019-0995-0.
[33] Z.J. Li, M. Feng, J. Zhang, X.Z. Wang, E. Xu, C. Wang, F.C. Lin, Z. Yang, H. Yu, W.X. Guan, H. Wang, WD40 repeat 43 mediates cell survival, proliferation, migration and invasion via vimentin in colorectal cancer, Cancer Cell Int. 21 (2021), https://doi.org/10.1186/s12935-021-02109-1. ARTN 418.
[34] S.B. Sondalle, S.J. Baserga, P.C. Yelick, The contributions of the ribosome biogenesis protein utp5/WDR43 to craniofacial development, J. Dent. Res. 95 (2016) 1214–1220, https://doi.org/10.1177/0022034516651077.
[35] J.-X. Lin, X.-S. Xie, X.-F. Weng, S.-L. Qiu, C. Yoon, N.-Z. Lian, J.-W. Xie, J.-B. Wang, J. Lu, Q.-Y. Chen, L.-L. Cao, M. Lin, R.-H. Tu, Y.-H. Yang, C.-M. Huang, C.-H. Zheng, P. Li, UFM1 suppresses invasive activities of gastric cancer cells by attenuating the expres7sion of PDK1 through PI3K/AKT signaling, J. Exp. Clin. Cancer Res. 38 (2019) 410, https://doi.org/10.1186/s13046-019-1416-4.
[36] S.Y. Bae, S. Byun, S.H. Bae, D.S. Min, H.A. Woo, K. Lee, TPT1 (tumor protein, translationally-controlled 1) negatively regulates autophagy through the BECN1 interactome and an MTORC1-mediated pathway, Autophagy 13 (2017) 820 833, https://doi.org/10.1080/15548627.2017.1287650.
[37] W. Abbas, A. Kumar, G. Herbein, The eEF1A proteins: at the crossroads of oncogenesis, apoptosis, and viral infections, Front. Oncol. 5 (2015), https://doi.org/10.3389/fonc.2015.00075. ARTN 75.
[38] Y. Pu, Y.Q. Liu, Y. Zhou, Y.F. Qi, S.P. Liao, S.K. Miao, L.M. Zhou, L.H. Wan, Dual role of RACK1 in airway epithelial mesenchymal transition and apoptosis, J. Cell Mol. Med. 24 (2020) 3656–3668, https://doi.org/10.1111/jcmm.15061.
[39] S. Rain, M.L. Handoko, P. Trip, C.T.J. Gan, N. Westerhof, G.J. Stienen, W.J. Paulus, C.A.C. Ottenheijm, J.T. Marcus, P. Dorfmuller, C. Guignabert, M. Humbert, P. MacDonald, C. dos Remedios, P.E. Postmus, C. Saripalli, C.G. Hidalgo, H.L. Granzier, A. Vonk-Noordegraaf, J. van der Velden, F.S. de Man, Right ventricular diastolic impairment in patients with pulmonary arterial hypertension, Circulation 128 (2013) 2016–2025, https://doi.org/10.1161/Circulationaha.113.001873.
[40] Y.G. Yuan, C.Y. Zhao, X.F. An, L. Wu, H. Wang, M. Zhao, M. Bai, S.Y. Duan, B. Zhang, A.H. Zhang, C.Y. Xing, A vital role for myosin-9 in puromycin aminonucleoside-induced podocyte injury by affecting actin cytoskeleton, Free Radical Res 50 (2016) 627–637, https://doi.org/10.3109/10715762.2016.1155706.
[41] A. Ghaffari, V. Hoskin, G. Turashvili, S. Varma, J. Mewburn, G. Mullins, P.A. Greer, F. Kiefer, A.G. Day, Y. Madarnas, S. SenGupta, B.E. Elliott, Intravital imaging reveals systemic ezrin inhibition impedes cancer cell migration and lymph node metastasis in breast cancer, Breast Cancer Res. 21 (2019), https://doi.org/10.1186/s13058-018-1079-7. ARTN 12.
[42] R. Li, P. Li, J. Wang, J. Liu, STIP1 down-regulation inhibits glycolysis by suppressing PKM2 and LDHA and inactivating the Wnt/β-catenin pathway in cervical carcinoma cells, Life Sci. 258 (2020) 118190, https://doi.org/10.1016/j.lfs.2020.118190.
[43] Y. Xia, J. Chen, G. Liu, W. Huang, X. Wei, Z. Wei, Y. He, STIP1 knockdown suppresses colorectal cancer cell proliferation, migration and invasion by inhibiting STAT3 pathway, Chem. Biol. Interact. 341 (2021) 109446, https://doi.org/10.1016/j.cbi.2021.109446.
[44] P.X. Gao, K. Zou, L. Xiao, H.X. Zhou, X.P. Xu, Z.G. Zeng, W. Zhang, High expression of PTGES3 is an independent predictive poor prognostic biomarker and correlates with immune infiltrates in lung adenocarcinoma, Int. Immunopharm. 110 (2022), https://doi.org/10.1016/j.intimp.2022.108954. ARTN 108954.
[45] Y.C. Wang, D.Y. Chen, H. Xie, M.W. Jia, X.F. Sun, F. Peng, F.F. Guo, D.L. Tang, AUF1 protects against ferroptosis to alleviate sepsis-induced acute lung injury by regulating NRF2 and ATF3, Cell. Mol. Life Sci. 79 (2022), https://doi.org/10.1007/s00018-022-04248-8. ARTN 228.
[46] Y. Dong, D. Ding, J. Gu, M. Chen, S. Li, Alpha-2 Heremans Schmid Glycoprotein (AHSG) promotes the proliferation of bladder cancer cells by regulating the TGF-β signalling pathway, Bioengineered 13 (2022) 14282–14298, https://doi.org/10.1080/21655979.2022.2081465.
[47] M. Zhou, H.H. Simms, P. Wang, Adrenomedullin and adrenomedullin binding protein-1 attenuate vascular endothelial cell apoptosis in sepsis, Ann. Surg. 240 (2004) 321–330, https://doi.org/10.1097/01.sla.0000133253.45591.5b.
[48] J.A. Seo, M.C. Kang, W.M. Yang, W.M. Hwang, S.S. Kim, S.H. Hong, J.I. Heo, A. Vijyakumar, L.P. de Moura, A. Uner, H. Huang, S.H. Lee, I.S. Lima, K.S. Park, M. S. Kim, Y. Dagon, T.E. Willnow, V. Aroda, T.P. Ciaraldi, R.R. Henry, Y.B. Kim, Apolipoprotein J is a hepatokine regulating muscle glucose metabolism and insulin sensitivity, Nat. Commun. 11 (2020), https://doi.org/10.1038/s41467-020-15963-w. ARTN 2024.
[49] M.R. Lee, G.H. Lee, H.Y. Lee, D.S. Kim, M.J. Chung, Y.C. Lee, H.R. Kim, H.J. Chae, BAX inhibitor-1-associated V-ATPase glycosylation enhances collagen degradation in pulmonary fibrosis, Cell Death Dis. 5 (2014) e1113, https://doi.org/10.1038/cddis.2014.86.
[50] A.J. Osband, E.A. Deitch, C.J. Hauser, Q. Lu, S. Zaets, T. Berezina, G.W. Machiedo, K.K. Rajwani, D.Z. Xu, Albumin protects against gut-induced lung injury in vitro and in vivo, Ann. Surg. 240 (2004) 331–339, https://doi.org/10.1097/01.sla.0000133359.12284.6b.
[51] K.A. Powers, A. Kapus, R.G. Khadaroo, R. He, J.C. Marshall, T.F. Lindsay, O.D. Rotstein, Twenty-five percent albumin prevents lung injury following shock/resuscitation, Crit. Care Med. 31 (2003) 2355–2363, https://doi.org/10.1097/01.CCM.0000084846.45830.AA.
[52] G.J. Quinlan, S. Mumby, G.S. Martin, G.R. Bernard, J.M. Gutteridge, T.W. Evans, Albumin influences total plasma antioxidant capacity favorably in patients with acute lung injury, Crit. Care Med. 32 (2004) 755–759, https://doi.org/10.1097/01.ccm.0000114574.18641.5d.
[53] R.H. Demling, Smoke inhalation lung injury: an update, Eplasty 8 (2008) e27.
[54] R.L. Mueller, S. Scheidt, History of drugs for thrombotic disease. Discovery, development, and directions for the future, Circulation 89 (1994) 432–449, https://doi.org/10.1161/01.cir.89.1.432.
[55] R.A. Greenfield, B.R. Brown, J.B. Hutchins, J.J. Iandolo, R. Jackson, L.N. Slater, M.S. Bronze, Microbiological, biological, and chemical weapons of warfare and terrorism, Am. J. Med. Sci. 323 (2002) 326–340, https://doi.org/10.1097/00000441-200206000-00005.
[56] P.H. Whitaker, Radiological appearances of the chest following partial asphyxiation by a smoke screen, Br. J. Radiol. 18 (1945) 396, https://doi.org/10.1259/0007-1285-18-216-396.
[57] Z. Xie, J. Dai, L. Dai, M. Tan, Z. Cheng, Y. Wu, J.D. Boeke, Y. Zhao, Lysine succinylation and lysine malonylation in histones, Mol. Cell. Proteomics 11 (2012) 100–107, https://doi.org/10.1074/mcp.M111.015875.
[58] K. Kurmi, S. Hitosugi, E.K. Wiese, F. Boakye-Agyeman, W.I. Gonsalves, Z.K. Lou, L.M. Karnitz, M.P. Goetz, T. Hitosugi, Carnitine palmitoyltransferase 1A has a lysine succinyltransferase activity, Cell Rep. 22 (2018) 1365–1373, https://doi.org/10.1016/j.celrep.2018.01.030.
[59] J.A. Boylston, J. Sun, Y. Chen, M. Gucek, M.N. Sack, E. Murphy, Characterization of the cardiac succinylome and its role in ischemia-reperfusion injury, J. Mol. Cell. Cardiol. 88 (2015) 73–81, https://doi.org/10.1016/j.yjmcc.2015.09.005.
[60] O. Peñuelas, J.A. Aramburu, F. Frutos-Vivar, A. Esteban, Pathology of acute lung injury and acute respiratory distress syndrome: a clinical-pathological correlation, Clin. Chest Med. 27 (2006).
[61] N. Yamamoto, O.K. Kan, M. Tatsuta, Y. Ishii, T. Ogawa, S. Shinozaki, S. Fukuyama, Y. Nakanishi, K. Matsumoto, Incense smoke-induced oxidative stress disrupts tight junctions and bronchial epithelial barrier integrity and induces airway hyperresponsiveness in mouse lungs, Sci. Rep. 11 (2021) 7222, https://doi.org/10.1038/s41598-021-86745-7.
[62] Q. Lu, P. Sakhatskyy, K. Grinnell, J. Newton, M. Ortiz, Y. Wang, J. Sanchez-Esteban, E.O. Harrington, S. Rounds, Cigarette smoke causes lung vascular barrier dysfunction via oxidative stress-mediated inhibition of RhoA and focal adhesion kinase, Am. J. Physiol. Lung Cell Mol. Physiol. 301 (2011) L847–L857, https://doi.org/10.1152/ajplung.00178.2011.
[63] P. Sakhatskyy, G.A. Gabino Miranda, J. Newton, C.G. Lee, G. Choudhary, A. Vang, S. Rounds, Q. Lu, Cigarette smoke-induced lung endothelial apoptosis and emphysema are associated with impairment of FAK and eIF2α, Microvasc. Res. 94 (2014) 80–89, https://doi.org/10.1016/j.mvr.2014.05.003.

[64] Y.H. Kim, M.K. Kang, E.J. Lee, D.Y. Kim, H. Oh, S.I. Kim, S.Y. Oh, W.J. Na, J.H. Shim, I.J. Kang, Y.H. Kang, Astragalin inhibits cigarette smoke-induced pulmonary thrombosis and alveolar inflammation and disrupts PAR activation and oxidative stress-responsive MAPK-signaling, Int. J. Mol. Sci. 22 (2021), https://doi.org/10.3390/ijms22073692. ARTN 3692.

[65] K. Murakami, P. Enkhbaatar, K. Shimoda, A. Mizutani, R.A. Cox, F.C. Schmalstieg, J.M. Jodoin, H.K. Hawkins, L.D. Traber, D.L. Traber, High-dose heparin fails to improve acute lung injury following smoke inhalation in sheep, Clin. Sci. (Lond.) 104 (2003) 349–356.

[66] R. Ren, Z. Ruan, H. Ding, J. Du, W. Yu, Phosphoproteome profiling provides insight into the mechanisms of ventilator-induced lung injury, Exp. Ther. Med. 19 (2020) 3627–3633, https://doi.org/10.3892/etm.2020.8634.